Sensors & Diagnostics

TUTORIAL REVIEW

View Article Online
View Journal | View Issue

Cite this: *Sens. Diagn.*, 2024, **3**, 28

Organic fluorophore-based fluorescent probes for abnormal immune response diagnosis and treatment evaluation

Shan Zuo, Yanhua Li, Tianbing Ren * and Lin Yuan *

Received 29th September 2023,
Accepted 13th November 2023

DOI: 10.1039/d3sd00259d

rsc.li/sensors

Real-time monitoring of the processes involved in abnormal immune responses can be used for the early diagnosis of immune system-related diseases (tumors, transplant rejection, autoimmune diseases, *etc.*), thus facilitating effective interventions. By purposefully combining organic small-molecule fluorescent probes with immune system-related molecules (enzymes/small-molecules), it is possible to visualize the activation status of relevant immune cells during abnormal immune processes, thus allowing timely adjustments to the immunotherapy regimen and improving the efficacy of immunotherapy. This paper summarizes the progress in the application of fluorescent probes based on small organic dyes for studying immune system-related processes and discusses the opportunities and challenges related to using fluorescent probes in monitoring immune system-related diseases and their treatments.

Introduction

The immune process *in vivo* is complex, involving a variety of functional cells (T cells, macrophages, cytotoxic lymphocytes, *etc.*), cytokines (IL-6, IL-2, IFN, TNF, *etc.*), and different mechanisms.[1–4] Abnormal immune function can seriously affect human life and health.[5] Usually, lower immune function in the body causes various diseases, including cancer.[6–9] However, when immune function is hyperactive, transplant rejection and a range of autoimmune diseases can occur.[5,10,11] In the last decade, immune system-related processes have received much attention, and more immune system-related biomarkers have been discovered and reported.[12,13] Therefore, to monitor and evaluate the immune status of the body, it is necessary and urgent to develop straightforward methods to monitor the fluctuation of immune system-related biomarkers in the body.[14]

At present, blood immunoassays, lymphocyte function examination and cytokine detection are the main methods for clinical detection of immunity in the body. Blood immunoassays include two main parts: immunoassay and serological examination. Immunoassays check the patient's antibody levels and immune cells. Serological tests involve measuring a variety of specific elements and indicators in the serum to assess a patient's immune system status. These indicators can reflect the overall condition of the patient's immune system.[15] Although effective, these methods suffer from low sensitivity and tedious preprocessing, and cannot reflect the immune system status of the body in real time.[16] By contrast, molecular imaging technologies including fluorescence imaging (FLI), magnetic resonance imaging (MRI), computed tomography (CT), and ultrasound imaging (USI) have shown higher sensitivity and real-time imaging ability for the study of immune processes.[17] In particular, FLI based on small-molecule probes has been the most important approach for *in vivo* real-time immune imaging, owing to its high spatiotemporal resolution, being a non-invasive detection method, low cost, and minimally toxic.[18,19] In addition, small-molecule probes can also be easily designed to be always-on, turn-on, turn-off and other different types of probe by regulating the fluorescent molecular structure to meet the evaluation needs of different immune processes.[20,21] Therefore, a large number of small-molecule fluorescent probes with distinct photophysical properties have been developed to date for *in vivo* study of the immune system.[22–26] Furthermore, researchers have also constructed some small-molecule fluorescent probes with excellent photodynamic and photothermal properties, which display great potential for the early diagnosis and intervention in immune abnormalities.

In this review, we will focus on advances in the use of organic fluorescent molecules to detect key biomarkers in various immune disorders (Fig. 1). First, we briefly introduce the abnormal immune processes and related *in vivo* diseases, and give an overview of the related intervention methods and

State Key Laboratory of Chemo/Biosensing and Chemometrics, College of Chemistry and Chemical Engineering, Hunan University, Changsha 410082, PR China.
E-mail: rentianbing@hnu.edu.cn, lyuan@hnu.edu.cn

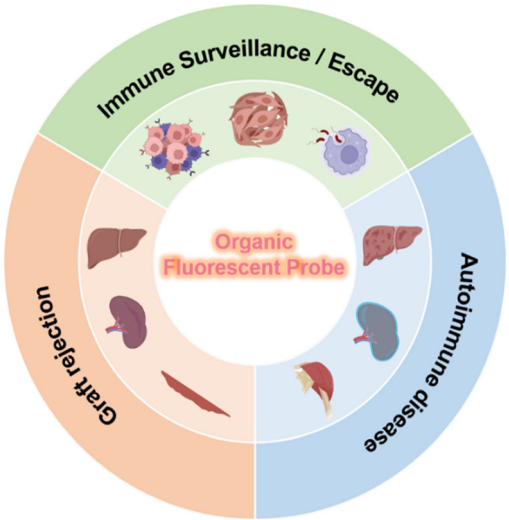

Fig. 1 Organic fluorescent probes can be used to image abnormal immune processes.

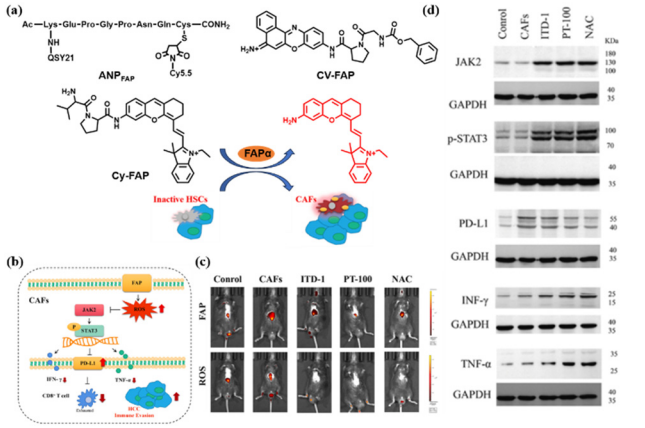

Fig. 2 (a) The mechanism by which **Cy-FAP** recognizes fibroblast activation protein (FAP). (b) Schematic diagram showing the mechanism underlying how CAFs promote the immune evasion of HCC. (c) 100 μL of a 50 μM **Cy-FAP** PBS solution (pH = 7.2–7.4) and 100 μL of 80 μM dihydroethidium (DHE) were administrated to orthotopic mouse models of HCC after treatment with saline (control), TGF-β (CAFs), ITD-1 (ITD-1), PT-100 (PT-100) and NAC (NAC). (d) Western blot analysis of JAK2, p-STAT3, PD-L1 TNF-α and IFN-γ in mice. Copyright© 2023 Elsevier B.V.

their efficacies. Then, we summarize the chemical structures of recently developed organic fluorescent probes and highlight their bioimaging and biosensing applications in abnormal immune processes and their treatments. Finally, we look at the current challenges and opportunities for the use of organic fluorescent probes in immune system related research, including in the early clinical diagnosis of immune diseases, imaging-guided interventions, and the prediction of treatment outcomes.

Probes targeting signaling molecules in abnormal immune processes

Immune homeostasis, which maintains the normal function of the body, involves complex mechanisms and both large signaling molecules (such as proteins, nucleic acids, polysaccharides, *etc.*) and small signaling molecules (such as reactive oxygen species, biological mercaptans, *etc.*).[1–4] When immune homeostasis is disrupted, the content and activity of signaling molecules change, triggering a downstream cascade that ultimately promotes the development of disease (tumor, inflammation, rejection).[9,27] Timely monitoring of these signaling molecules (especially enzymes and small molecules) with organic fluorescent probes/dyes can provide immune system information earlier and more accurately, which is very important for the early diagnosis and intervention in abnormal immune function.

Sensing of enzymes in abnormal immune processes

The dominant stromal cells in the tumor microenvironment (TME) are cancer-associated fibroblasts (CAFs) which promote the immune escape of hepatocellular carcinomas (HCC) by secreting fibroblast activation protein-α (FAPα).[28–30] Thus, monitoring the expression of FAPα can be used for the study of the immune escape of tumors. For example, in 2012, Cheng *et al.* designed the probe $\mathbf{ANP_{FAP}}$ by linking a near-infrared dye (Cy5.5) with a quencher dye (QSY21) *via* a short amino acid sequence specific to FAPα cleavage (KGPGPNQC) (Fig. 2a).[31] Due to effective fluorescence resonance energy transfer (FRET) between Cy5.5 and QSY21, the NIR fluorescence signal was significantly elevated after cutting the amino acid sequence with FAPα *in vitro* and *in vivo*. With this probe, the author realized high-contrast differentiation of C6 (glioma cells) tumor cells and U87MG (malignant glioma cells) tumor cells *via* detection of FAPα. Also, this result indicated that U87MG tumor cells, with a higher expression of FAPα, may exhibit more serious immune escape, thus inhibiting the immune clearance ability of the body and promoting the development of malignant brain glioma. In 2022, to achieve the effective diagnosis and treatment of melanoma (a serious tumor that threatens both life and health) at the same time, Nie *et al.* developed a novel organic fluorescent probe, **CV-FAP**, which contained a highly specific recognition unit (Z-Gly-Pro) and the red light-emitting fluorophore cresol violet[32] (Fig. 2a). Using **CV-FAP**, the authors not only realized the ultrasensitive detection of endogenous FAPα in living cells and in melanoma mice, but also obtained significant antitumor activity by activating an immune process in melanoma cells and tumor-bearing nude mice (inhibiting tumor growth by more than 95%). Recently, *via* an *in situ* fluorescence imaging strategy using probe **Cy-FAP**, Tang *et al.* found that, in an orthotopic mouse model, FAPα secreted by CAFs can cause drastic changes in the reactive oxygen species (ROS) in mice[33] (Fig. 2c). High levels of ROS production can lead to upregulation of PD-L1, down-regulation of TNF-α and IFN-γ, and promote the degree of immune escape of HCC (Fig. 2b and d). These results further verified that FAPα plays an important role in tumor immune

escape, which is crucial for a deep understanding of FAPα as an immune upregulation indicator of malignant tumors (Fig. 2b).

In contrast to CAFs, another immune abnormality, an inflammatory response, is primarily associated with the upregulation of the matrix metalloproteinase (MMP) and cathepsin families in macrophages.[34] Therefore, it is useful to assess the degree of immunity by monitoring the expression of these enzymes in inflammatory responses.[35] In 2006, Weissleder *et al.* designed and synthesized a FRET probe, NIRF-MMP, based on Cy5.5 and a quencher.[36] The linker in the probe is GGPRQITAG, a peptide substrate for MMP-2 and MMP-9 that targets overexpressed MMP-2 and MMP-9 in atherosclerosis. In the atherosclerosis model, the fluorescence signal of NIRF-MMP overlaps highly with the macrophage-specific marker (Mac3) signal, which strongly supports the development of arterial plaque through the secretion of MMP2/9 by macrophages. Similar to MMP enzymes, a large number of FRET organic fluorescent probes have been designed to detect the cathepsin released from macrophages in inflammatory responses. For example, in atherosclerosis, Weissleder *et al.* developed a probe, NIRF-CatK, with the GHPGGPQKC sequence as a linker which cathepsin K(CTSK) can specifically cleave.[37] NIRF-CatK was able to detect the high CTSK activity associated with elastin fiber breakage and massive macrophage infiltration in an experimental mouse model of atherosclerosis. It is noteworthy that NIRF-CatK also detected high cathepsin K activity in fresh human atherosclerosis samples, indicating that cathepsin K is closely associated with the immune processes related to inflammation. In addition to the above targets, researchers also designed fluorescent probes based on a FRET strategy for the detection of MMP12, MMP13, *etc.*, and used them in inflammatory immune responses involving macrophages.[38] However, one limitation of these FRET probes is their inherently large molecular weight, which is a challenge for the synthesis and fast imaging of metabolic rates.[34]

In addition to the involvement of macrophages, T lymphocytes (CTLs) and natural killer (NK) cells also play an important role in hyperimmune responses during inflammation.[39] In these two cells types, the granzymes, including granzyme A and granzyme B (GrA and GrB), are the main biomarkers for evaluating the degree of immunity.[40,41] At present, organic fluorescent probes have been effectively explored in autoimmune hepatitis (AIH), which is a classic activated T cell involvement process. For example, in 2022, Pu *et al.* designed and synthesized an organic small molecule polymer platform (**APN$_G$**) for real-time monitoring of overexpressed GrB in AIH mediated by concanavalin A (Con-A).[42] The platform consists of three parts: (1) a protease-reactive peptide brush; (2) a cascaded self-immolative linker; and (3) a caged fluorophore unit with a renal clearance moiety and/or a targeting moiety. Using this probe, they observed that, compared with mice in a saline-fed control group, the immunosuppressant group treated with cyclosporin A or the severely immunodeficient groups showed high fluorescence signals in the liver and kidney. This result demonstrated that **APN$_G$** can be used to monitor immune diseases mediated by activated T lymphocytes in real time and is consistent with clinical/preclinical measures (ALT, AST, TNF-α, IFN-γ, IL-2 and IL-6, *etc.*).

As a stable and superior organic polymer fluorescence platform, **APN$_G$** can not only monitor the immune response in autoimmune hepatitis, but also evaluate more complex substantive organ transplantation.[42] Orthotopic liver transplantation is the only option for patients with end-stage liver disease. However, allograft rejection remains a major complication after transplantation. Pu *et al.* used dark agouti (DA) rats and Lewis rats as donor and recipient, respectively, for allograft orthotopic liver transplantation. Compared with different control groups, **APN$_G$** was specifically activated only in the graft liver, producing CyCD and entering the urine through the kidney. In addition, immunofluorescent staining showed that CyCD signaling in the liver was observed 3 days after transplantation, which coincided with the time when **APN$_G$** showed a significant difference signal in the urine. These results suggest that GrB, an enzyme biomarker in the process of immune abnormalities, can provide good information about liver transplantation rejection, thus inspiring rejection monitoring in other transplantation procedures. Clinically, kidney transplantation is much more common than liver transplantation.[43] In 2023, Pu *et al.* designed probes, **AMPro$_N$** and **AMPro$_T$**, based on polycyclodextrin-modified HD dyes to monitor acute rejection mediated by neutrophils and activated T cells after renal related immune diseases, respectively[44] (Fig. 3a). Both neutrophil elastase (from neutrophils) and granzyme B/GGT (from cytotoxic T cells) were significantly upregulated in allogeneic renal transplantation compared with allograft renal transplantation (Fig. 3e). By using **AMPro$_N$** and **AMPro$_T$**, researchers could clearly see that the innate immune mechanism occurs earlier than the specific immune process in renal autoimmune diseases (Fig. 3b). It is worth mentioning that **AMpro**-based urinalysis not only detected the onset of acute renal allograft rejection (ARAR) 1 day earlier than histological injury, but also had the highest sensitivity of all detection methods (Fig. 3c, d and f). Similar to complex substantive organ transplants, skin graft rejection also needs to be monitored in real time. Earlier, in 2018, Gabriel A. Kwong *et al.* visualized overexpressed GrB in skin grafts using an organic nano fluorescent probe **X**.[45] **X** contained three parts: iron oxide nanoparticles (IONPs); polyethylene glycol (PEG); and the best lytic peptide of GrB (AIEFD|SG). The probe is sensitive to GrB cleavage, which cannot cross-cut by the clotting and complement cascade, and cannot promote complement activity. Compared with the homologous allograft mice, the allograft mice showed a strong fluorescence signal at the skin graft site, and this signal difference was also observed in subsequent bladder and urine imaging. This organic fluorescent tool provides highly sensitive and specific non-invasive detection of the

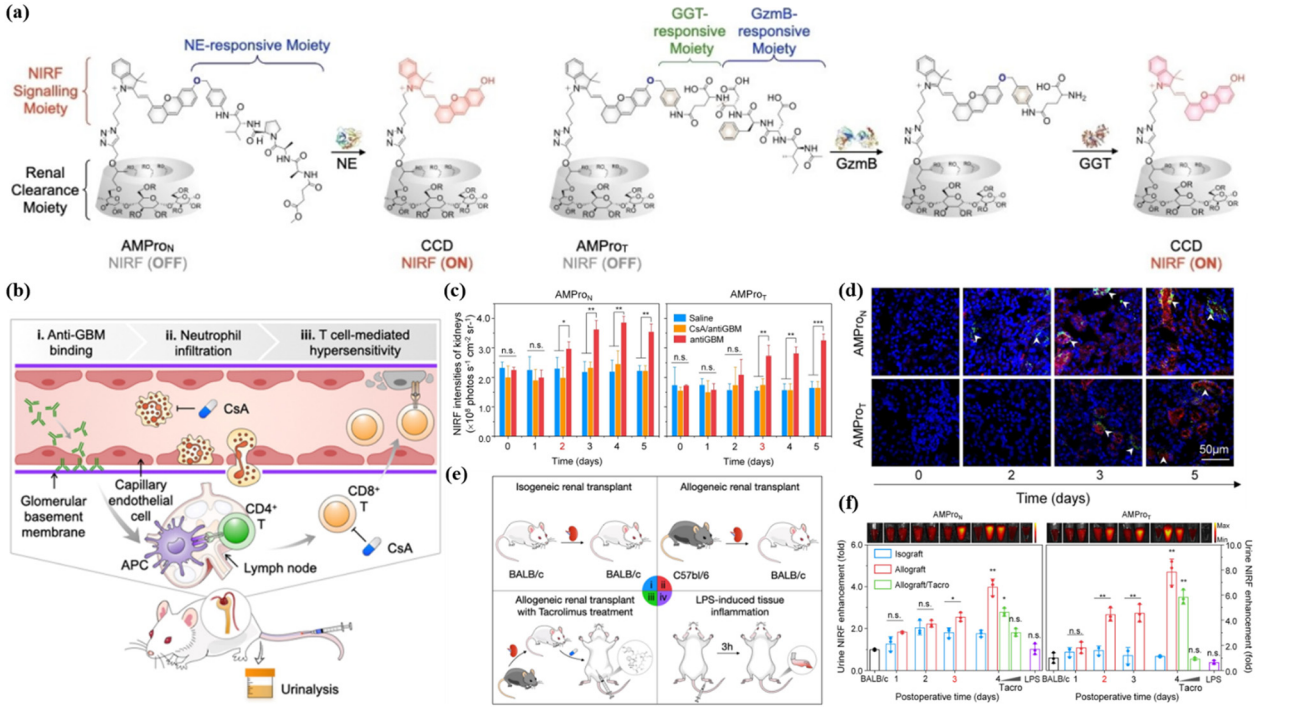

Fig. 3 (a) Chemical structures of **AMPro$_N$** and its activated form, CCD, after activation by neutrophil elastase, and **AMPro$_T$** and its activated form, CCD, after sequential activation by GrB and GGT. (b) Schematic illustration of how the **AMPro** probes detect the infiltrating neutrophils and CTLs *via* NIRF signal activation in an antiGBM-induced murine nephritis model. (c) NIRF intensities of kidneys in living mice t = 60 min after i.v. injection of **AMPro$_N$** and **AMPro$_T$** at different drug post-treatment time points (1, 2, 3, 4 or 5 days). (d) Representative confocal fluorescence microscopy images of regional kidney slices from mice i.v. injected with **AMPro$_N$** and **AMPro$_T$** at different drug post-treatment time points (0, 2, 3, 5 days). (e) Schematic illustration of established murine models, including isogeneic or allogeneic kidney transplant mice, allogeneic kidney transplant mice pre-treated with Tac, and LPS-induced tissue inflammation. (f) Relative NIRF enhancement of activated CCD in mice urine 6 h after injection of **AMPro$_N$**, **AMPro$_T$** (6.5 μmol kg^{-1} bw) for different treatment groups as compared to control.

occurrence of acute rejection reaction (ACR), avoids secondary damage compared to the conventional gold standard of ACR (invasive biopsy), and dynamically monitors the effect of immunosuppressive drug therapy.

Sensing of small molecules in abnormal immune processes

In addition to aiding the monitoring of fluctuations in enzyme levels, small molecule active substances such as ROS and reactive sulfur species (RSS), *etc.*, are also very important indicators of immune homeostasis.[46–48] It is well known that there is a high level of ROS and RSS in the tumor microenvironment, which pose a threat to the survival of immune cells.[5] In addition, the abnormal pH environment also affects the secretion and activity of relevant signaling macromolecules.[49] In 2021, Zhao *et al.* synthesized a ratio type near-infrared photoacoustic probe APSel which can be activated by selenol (a type of RSS) to detect relevant AIH processes.[50] The probe was composed of a near-infrared cyanine dye and a selenol-responsive group bis (2-hydroxyethyl) disulfide (Fig. 4a). The selenium–sulfur exchange reaction between APSel and selenol (Sec was used here) caused the release of the responsive group in the APSel molecule, which resulted in a blue shift of the PA spectrum peak from 860 nm to 690 nm (Fig. 4b and c). Using this probe, disease development was successfully monitored in a ConA-induced AIH mouse model by tracking changes in selenol levels (Fig. 4d–f).

Although the pathogenesis is still unclear, studies have shown that oxidative stress is a significant feature of rheumatoid arthritis (RA). During RA, macrophages are stimulated by pathogens and their peroxidase (MPO) is secreted into the phagosome and catalyzes HOCl production.[51] Therefore, there has been a lot of work on the early detection of RA with HOCl as the target. In 2017, Yi *et al.* designed **FDOCl-1** based on a new deformylation reaction.[52] The absorbance of **FDOCl-1** at 664 nm was increased by 577 times and the fluorescence intensity at 686 nm was increased by 2068 times after the addition of 2.5 equivalents of HOCl (Fig. 5b and c). This is undoubtedly very advantageous for fast and high contrast imaging of RA. Compared with the control group, the arthritic area in RA mice rapidly showed intense fluorescence in the near infrared range within 5 s (Fig. 5d and e). These findings show for the first time that **FDOCl-1** can detect arthritis-dependent HOCl production in the body using fluorescence imaging. Compared with NIR I, the NIR II organic fluorescence

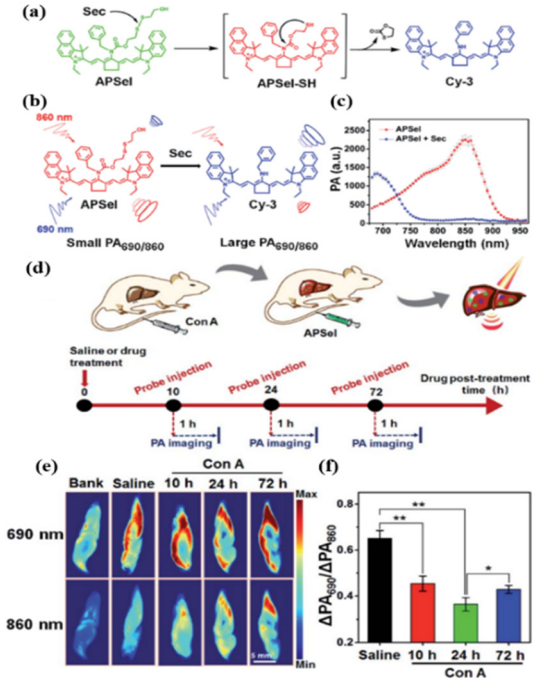

Fig. 4 (a) Schematic diagram of the reaction of the APSel probe with Sec. (b) Principle of ratiometric PA detection of Sec. (c) PA spectra of APSel solution in the presence or absence of Sec. (d) Schematic illustration of the monitoring of the pathological progression of AIH using the PA probe. (e) Representative *ex vivo* PA images of isolated livers from mice under different conditions. (f) The changes in the $\Delta PA_{690}/\Delta PA_{860}$ value in the livers of mice under different conditions. Copyright© 2021 The Royal Society of Chemistry.

probe has the advantages of minimizing self-fluorescence, higher spatial resolution and deeper body penetration, which is very favorable for the early diagnosis of RA. In 2021, Xiong *et al.* developed a new water-soluble "OFF–ON" NIR-II fluorescent probe, **PTA**, for tracking and imaging HClO in RA[53] (Fig. 5a). **PTA** responds quickly to HClO and turns on strong NIR-II fluorescence within 30 s, which is undoubtedly beneficial for detecting the early accumulation of HClO in RA. In particular, **PTA** was able to sensitively and rapidly visualize endogenous HClO in inflammatory RA mouse models by utilizing NIR-II fluorescence. In addition to HClO, $ONOO^-$ is also an overexpressed signaling molecule during RA development that is directly involved in tissue damage in patients with RA. Therefore, in 2022, Ding and Zhang *et al.* designed and synthesized a near-infrared fluorescent probe, **Lyso-Cy**, based on CS dyes that responded sequentially to pH and $ONOO^-$ (ref. 54) (Fig. 5a). Due to the lower pH (4.5–5.5) in the lysosome, the helical ring opens when **Lyso-Cy** enters the cell, producing a significant near-infrared emission at 745 nm. Further, the strong oxidation of $ONOO^-$ leads to the breaking of the carbon–carbon double bond, and the reduced conjugate skeleton leads to a blue shift of the emission wavelength. This double-reactive receptor was shown to be suitable for mouse models experiencing RA with a proportional response.

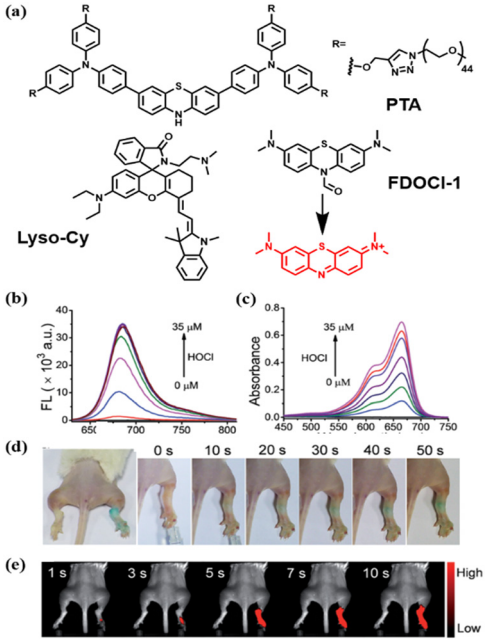

Fig. 5 (a) Structures of the HOCl probes. (b) Fluorescence and (c) absorption spectra of FDOCl-1 (10 mM in 10 mM PBS, pH 7.2) in the presence of different concentrations of HOCl. (d) *In vivo* images of the mouse model of arthritis. Colour changes observed by the naked eye more than 2 min after injection of FDOCl-1 and 0–50 s after injection of FDOCl-1. (e) Fluorescence images taken 1–10 s after injection of FDOCl-1. Copyright© 2018 The Royal Society of Chemistry.

Probe for signaling molecules during abnormal immune function treatment

Abnormal immune processes can seriously affect life and health, so timely and reasonable interventions (such as immunotherapy and immunosuppressant drugs) are very important. Tumor immune interventions include immune checkpoint blockers, adoptive cell therapy, *etc.*, while immunosuppressants are mainly used for hyperimmune responses (transplant rejection, autoimmune disease, *etc.*).[55] To date, organic fluorescent probes have been used for therapeutic evaluation by monitoring enzymes and small molecules associated with the intervention.

Sensing of enzyme in abnormal immune function intervention

GrB, an important serine protease in the immune process, has received extensive attention[56–59] because it can induce caspase-dependent and independent apoptosis in target cells, and it can directly act on death substrates producing cytotoxic effects.[60–63] Therefore, to achieve efficient killing of malignant tumor cells, a variety of ways to stimulate the expression of granzyme B have been adopted by researchers.[64] At the same time, many high-performance fluorescent probes have also been developed to monitor GrB expression during this process and guide tumor treatment.

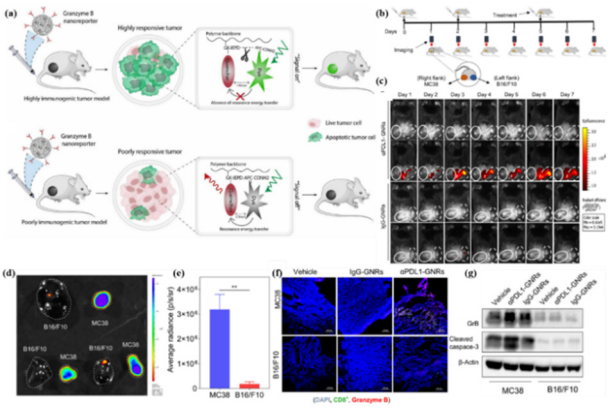

Fig. 6 (a) GrB-mediated fluorescence activation allows direct visualization of the T cell activity in the tumor and can be used to distinguish between immune-responsive and poorly responsive tumors. (b) Schematic representing GNR treatment schedule and animal imaging timeline. (c) Representative bright-field and fluorescence images of MC38 (dotted oval) and B16/F10 (solid oval) tumors in mice from different GNR treatment groups. (d) Representative NIR fluorescence image of excised MC38 and B16/F10 tumors after a single dose of aPDL1-GNR treatment on day 14 after tumor inoculation; tumors were excised after 48 hours of treatment. (e) Quantification of fluorescent signal from (d). (f) Representative confocal images of cross section of excised MC38 and B16/F10 tumors from different treatment groups. (g) Western blot analysis shows expression of GrB and cleaved caspase-3 in representative B16/F10 and MC38 tumors from different treatment groups. Copyright© 2020 Science.

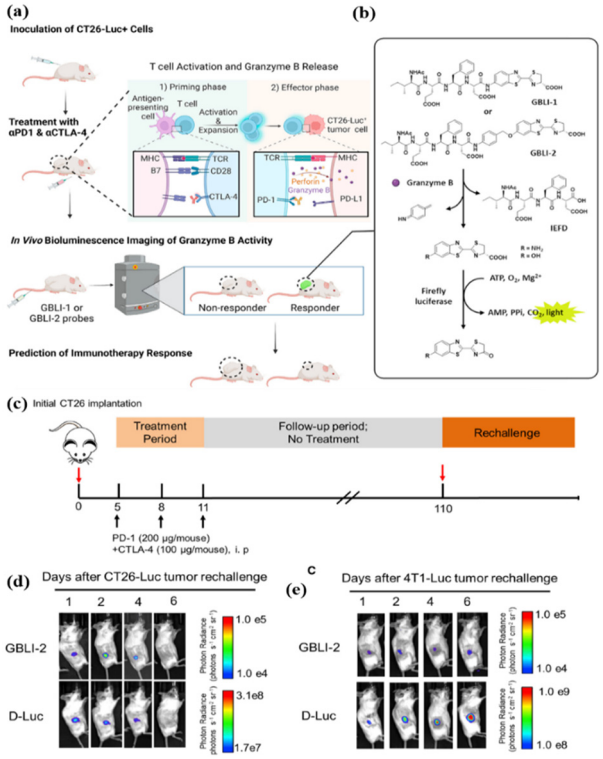

Fig. 7 (a) BALB/c mice bearing CT26-Luc+ tumors are treated with checkpoint inhibitors (anti-PD-1/ CLTA-4 antibodies) to block the inhibitory signaling toward cytotoxic T lymphocytes during both the (1) priming and (2) effector phases to induce a systemic immune response and release granzyme B to kill cancer cells. (b) In responders, the discharged granzyme B from CTLs cleaves the GBLI probe to generate free luciferins, which will be processed by firefly luciferase in CT26-Luc+ cells to emit bioluminescence. (c) Scheme showing the rechallenge experimental design to evaluate the immune memory effect *in vivo*. (d and e) Dynamic BLI images of rechallenged mice with CT26-Luc or 4T1-Luc cells taken after 6 days. Copyright© 2022 Elsevier Ltd.

In 2020, Ashish *et al.* designed a delivery imaging system (GNR) that can simultaneously deliver immunotherapy drugs and track the activity of T-cell-mediated GrB in real time.[65] GNR consists of three parts: a PIMA polymer backbone, anti-PD-L1 immune checkpoint antibodies conjugated to PEG linkers, and a NIR FRET pair conjugated on either side of a GrB peptide substrate (–IEPD-). Synchronous spatiotemporal distribution of fluorescence signals for monitoring and treatment can be obtained by delivering PD-L1 inhibitors and GrB-activated probes through this single nanocarrier (Fig. 6a). GNR was able to distinguish between responsive and non-responsive tumors in mice flanked with MC38 (colorectal adenocarcinoma cells) and B16/F10 (melanoma cells) cells (Fig. 6b). Only MC38 tumors treated with aPDL1-GNR showed obvious fluorescence signals, indicating that PD-L1-mediated immunotherapy can effectively improve the infiltration of CTL cells in MC38 tumors and release more functional GrB (Fig. 6c–g). This result confirms the reliability of activated GrB imaging as an early detection immune checkpoint inhibitor and can be used for longitudinal imaging of immunotherapy responses.

Similarly, immune checkpoint blockers for CTLA-4 have also been developed to remove the effects of T cell inhibition.[66] In 2022, Rao *et al.* reported a bioluminescent probe (GBLI-2) for noninvasive, real-time, longitudinal imaging of GrB activity in tumors receiving immune checkpoint inhibitors (PD-L1 and CTLA-4).[67] GBLI-2 was evaluated for imaging the dynamics of the GrB activity and predicting the therapeutic efficacy in a syngeneic mouse model of CT26 murine colorectal carcinoma (Fig. 7c). Notably, GBLI-2 successfully evaluated immunotherapy memory effects by not intervening at 100 days after co-treatment with PD-1 and CTLA-4, re-establishing subcutaneous tumors at 110 days, and monitoring tumor immunity and tumor growth again (Fig. 7d and e).

In addition to classical PD-L1/CTLA-4 immune checkpoint blocking therapy, adoptive cell immunotherapy can also be evaluated with a GrB-activatable organic fluorescent probe.[68,69] In 2020, Marc Vendrell *et al.* reported a GrB-specific probe, probe 1, based on phenoxydioxane chemiluminescent groups that have a higher signal-to-noise ratio against active GrB compared to commercial fluorescent probes (coumarin-structured)[70] (Fig. 8a–c). Further, the probe was used to visualize the adoptive NK cell recognition of tumors in a preclinical mouse model (Fig. 8d and e).

The organic optical probes designed by Rao and Marc *et al.* demonstrate highly sensitive detection capabilities, but

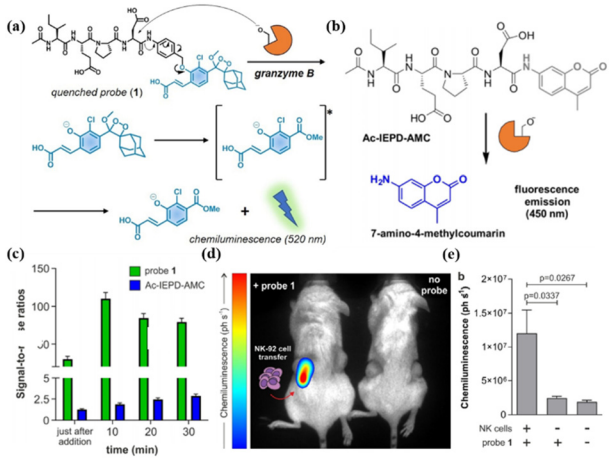

Fig. 8 (a) Activation mechanism of chemiluminescent probe 1. (b) Structure and activation mechanism of fluorogenic probe, Ac-IEPD-AMC. (c) Time-course signal-to-noise ratios after probe 1 (green bars, 100 mM) and Ac-IEPD-AMC (blue bars, 25 mM) were independently incubated with GrB (20 nM) in aqueous buffer at 37 °C. (d) Representative *in vivo* chemiluminescence images of NSG mice containing MDA-MB-231-xenograft tumors where NK-92 cells were adoptively transferred. (e) Quantification of chemiluminescence emission for each condition displayed. Copyright© 2021 Wiley-VCH GmbH.

have limitations for the long-term imaging of complex immune interventions *in vivo* due to the short wavelength, low energy, and short lifetime of the bio-chemiluminescence.

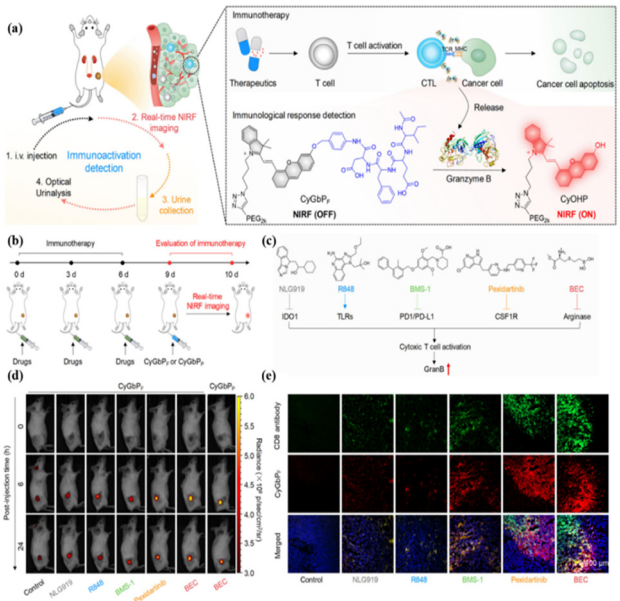

Fig. 9 (a) Optical urinalysis and mechanism for fluorescence imaging of CyGbPF. (b) Schematic illustration of the timeline of immunotherapy and real-time NIRF imaging. (c) Chemical structures of different immunotherapeutics for activation of immune responses. (d) Representative NIRF images of 4T1 tumor-bearing mice after i.v. injection of CyGbPF or CyGbPP (10 μmol kg^{-1}) into the mice treated with different immunotherapeutics. (e) Representative confocal fluorescence images of tumor sections of immunotherapeutic-treated mice at the end of real-time tracking. Copyright© 2020 American Chemical Society.

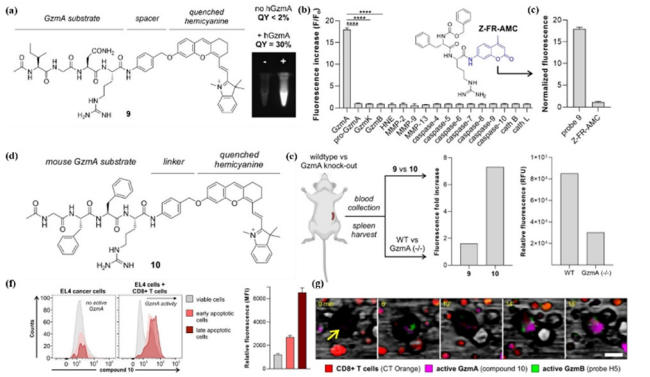

Fig. 10 (a) Pictograms of solutions of compound **9** (50 μM) in the absence (left) or presence (right) of hGrA under 650 nm excitation. (b) Increase in fluorescence of compound **9** (20 μM) after incubation with different proteases (all at 20 nM) at 37 °C for 60 min. (Inset) Chemical structure of commercially available Z-FR-AMC. (c) Enhancement of the fluorescence of compound **9** and Z-FR-AMC (both at 20 μM) after incubation with hGrA (20 nM) in Tris buffer (pH 8) at 37 °C for 60 min. (d) Chemical structure of compound **10**. (e) Fluorescence emission signals (λ_{exc}: 680 nm) from two independent experiments including sera from septic mice incubated with compounds **9** and **10** (both at 20 nM, left panel) and spleen lysates from infected wild-type (WT) mice and infected GrA knock-out mice after incubation with compound **10** (20 nM, right panel). (f) Representative histograms from flow cytometric analysis of EL4 cancer cells before and after co-culture with CD8+ T cells and incubation with compound **10** (2.5 μM). (g) Representative snapshots of time-lapse fluorescence microscopy of live cocultures of CD8+ T cells (red, counterstained with CellTrackerTM Orange) and EL4 cancer cells (yellow arrow) where GrA (compound **10**, magenta, 3 μM) and GrB (probe H5, green, 2.5 μM) activities were monitored upon antigen-driven interaction. Copyright© 2022 Wiley-VCH GmbH.

In 2020, Pu *et al.* designed renal-clearable near-infrared fluorescent probes (**$CyGbP_F$** and **$CyGbP_P$**) based on classical HD dyes that can evaluate the intervention effects of multiple immune-activating drugs online/offline over a long period of time (24 h)[71] (Fig. 9).

In addition to GrB, the importance of GrA in the immune process has also been gradually gaining more attention from researchers.[72] In 2023, Vendrell *et al.* reported the rational design of near-infrared fluorescent substrates for human GrA and mouse GrA.[73] By screening stable *p*-aminobenzyl alcohols in the physiological environment, the tetrapeptide sequence (Ac-Ile-Gly-Asn-Arg) was connected with HD dye to obtain probe **9** (Fig. 10a). Encouraged by the high performance of the response of probe **9** to GrA (Fig. 10b), Marc *et al.* used probe **10** (rat GrA) for real-time multiplex imaging of granzyme activity in the co-culture of cancer cells and adaptive immune cells (Fig. 10d). Real-time images showed an almost simultaneous burst of activity of both enzymes in EL4 cancer cells, suggesting that CTLs can stimulate the activity of GrA and GrB in response to antigen-driven recognition (Fig. 10f and g). This suggests that monitoring GrA fluctuations in tumor immunotherapy is also important.

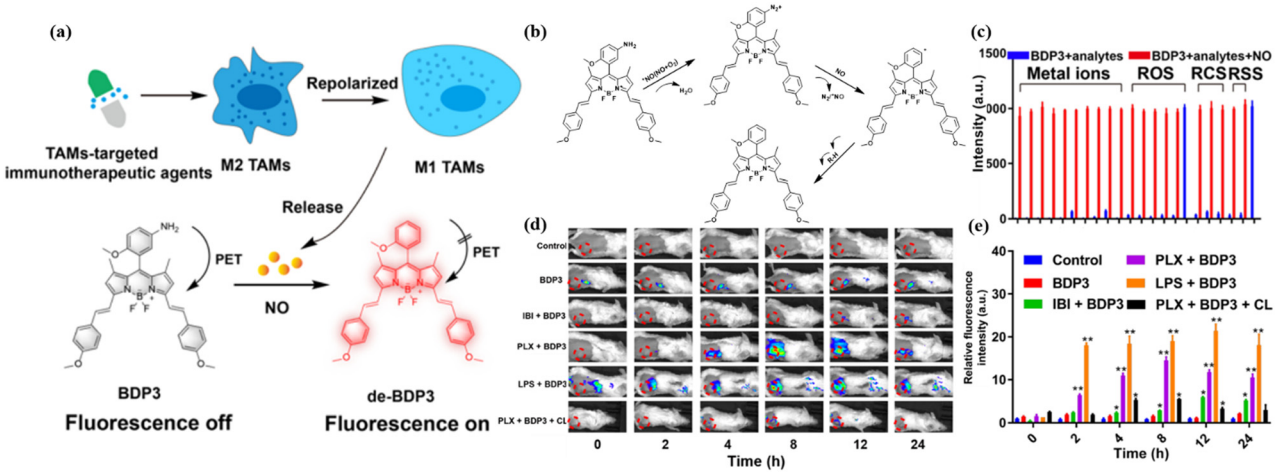

Fig. 11 (a) Schematic illustration of the detection of the therapeutic efficiency of immunotherapeutic drugs. (b) Reaction mechanism of **BDP3** with NO in aerobic conditions. (c) Fluorescence intensities of BDP3 (5 μM) treated with various metal ions (1: Na^+, 2: K^+, 3: Cu^+, 4: Zn^{2+}, 5: Cu^{2+}, 6: Fe^{2+}, 7: Ca^{2+}, 8: Al^{3+}, 9: Fe^{3+}, 10: Mg^{2+}), ROS (11: HO·, 12: $O_2^{\cdot-}$, 13: $^1O_2$, 14: H_2O_2, 15: ClO^-, 16: $ONOO^-$), RCS (17: formaldehyde, 18: ascorbic acid, 19: methylglyoxal), and RSS (20: Cys, 21: GSH), and NO (22). (d) Confocal images of M2 phenotype RAW 264.7 cells treated with IBI (1 μg mL^{-1}) or PLX (1 μg mL^{-1}) for different time intervals and stained with BDP3. Images (d) and quantitative analysis (e) of the relative fluorescence intensities of 4T1-bearing mice following different treatments and compared with control groups. Copyright© 2023 American Chemical Society.

Sensing of small molecules in abnormal immune function intervention

In the course of abnormal immune function treatment, although granzymes (mainly GrB) are the specific enzymes used for evaluating immune response,[74] some small molecules can also provide a wealth of immune system-related information.[75]

Immunomodulation of tumor-associated macrophages (TAMs) from a protumorigenic phenotype (M2) to an antitumorigenic phenotype (M1) is crucial in macrophage-targeted immunotherapy.[76] Compared with M2 macrophages, M1 macrophages have a higher level of NO. In 2020 and 2023, Ashish Kulkarni and Gao *et al.* designed probes NO-NR and BDP3 for monitoring NO in M1 based on different fluorescent organic structures.[77,78] A hydrophobic amphiphile, iCSF1R, occupies the spaces between the lipid bilayer along with the NO imaging probe (DAF-2-DA), thereby constituting an immunotheranostic system, iCSF1R–NO-NR. The most significant enhancement of the fluorescence signal was observed in the iCSF1R-NO-NR group in a mouse 4T1 breast cancer model. It is worth noting that DAF-2-DA can also react with $ONOO^-$ to emit high brightness fluorescence, which is very unfavorable for accurately reporting NO information in the TME. Moreover, the DAF-2-DA wavelength is located in the visible region and is not conducive to the long-term live imaging required for deeper penetration. Compared to probe DAF-2-DA, BDP3 developed by the Guo group not only specifically activates stable and sensitive fluorescence of NO *via* a photoinduced electron transfer (PET) process but also achieves a long emission wavelength for efficient *in vitro* and *in vivo* imaging (Fig. 11a). As reported by Guo *et al.*, the response mechanism of BDP3 is shown in Fig. 11b.[79] The different effects on two clinically used immunotherapy agents further confirm the ability of BDP3 to specifically monitor M1/M2 switches in macrophage targeted immunotherapy responses (Fig. 11d and e). However, BDP3 still failed to eliminate $ONOO^-$ interference with its fluorescence signal (Fig. 11c), which needs to be addressed further.

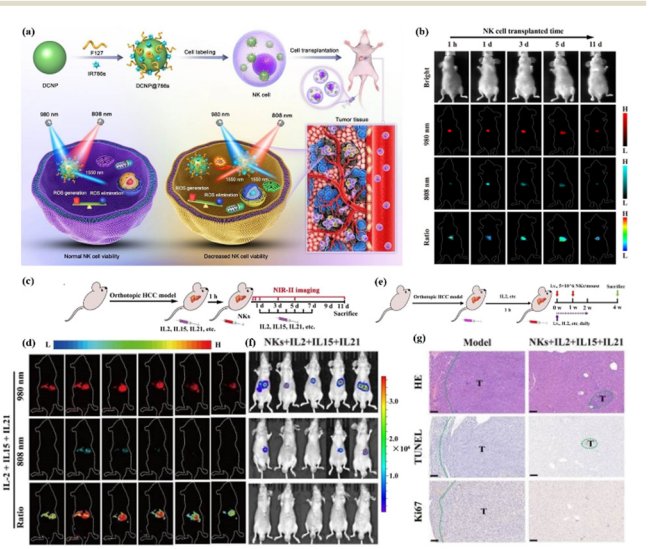

Fig. 12 (a) Schematic illustration of the use of DCNP@786 s for ratiometric NIR-II fluorescent imaging for tracking NK cell viability *in vivo*. (b) Ratiometric NIR-II fluorescence images taken 1 h, 1 d, 3 d, 5 d, and 11 d after NK cell transplantation. (c) Schematic illustration of co-treatment of IL-2, IL-15, and IL-21 for enhancing NK cell viability in an orthotopic HCC model. (d) Ratiometric NIR-II fluorescence images taken 1 h, 1 d, 3 d, 5 d, and 11 d after NK cell transplantation. (e) Schedule co-treatment of IL-2, IL-15, and IL-21 for NK cell-based immunotherapy. (f) Chemiluminescence images following different treatments. (g) HE-, TUNEL- and Ki67-staining of tumor tissues following different treatments. Copyright© 2021 Wiley-VCH GmbH.

Table 1 Table showing full text of abbreviated nouns

Full name	Abbreviation
Fluorescence imaging	FLI
Magnetic resonance imaging	MRI
Computed tomography	CT
Ultrasound imaging	USI
Granzyme A/granzyme B	GrA/GrB
Concanavalin A	Con-A
Dark agouti	DA
Rheumatoid arthritis	RA
Tumor-associated macrophages	TAMs
Matrix metalloproteinase	MMP

In addition to directly imaging specific small molecular markers of tumor-associated immune cells, labeling adoptive NK cells with organic dyes to assess their active status and therapeutic status can also be achieved by monitoring ROS levels. In 2021, Song *et al.* developed a quantitative NIR-II fluorescence imaging probe, DCNP, to quantitatively track and visualize adoptive NK cell viability *in vivo* in real time[80] (Fig. 12a). The nanoprobe consists of lanthanide down-converted nanoparticles coated with IR786s, a reactive oxygen species (ROS) sensitive to near-infrared dyes, and labeled directly with NK cells. During cell death, excess ROS was generated in the NK cells, accompanied by degradation of IR786s. Thus, the fluorescence signal of NIR-II was turned on at 1550 nm under 808 nm excitation, while the fluorescence signal was stable at 980 nm. The NIR II signal ratio of activated DCNP correlates well with the survival of NK cells *in vitro* and *in vivo* (hepatocellular carcinoma model) (Fig. 12b). More notably, real-time monitoring by DCNP has proved that the combined treatment of IL-2, IL-15 and IL-21 can improve the survival rate of NK cells and the efficiency of cell transplantation *in vivo*, as well as the treatment efficiency of orthotopic hepatocellular carcinoma (Fig. 12c–g).

Conclusions and outlook

Abnormal immune processes in the body often involve complex pathways. Abnormal immune processes promote tumor development, autoimmune inflammation, and acute transplant rejection, which can be a serious threat to life and health. The occurrence of these diseases is mainly mediated by major macromolecular proteins such as serine protease (granzymes), cysteine protease (cathepsins), and metalloproteinase (MMPs) and also by redox mechanisms. Existing monitoring methods have some problems, such as being invasive, time-consuming, and having low sensitivity. Fluorescent dyes and probes can effectively play a role in the monitoring of abnormal immune processes due to their characteristics of giving data in real time, being non-invasive and being highly sensitive. Thus, a well-designed fluorescent probe can effectively monitor tumors, autoimmune diseases and transplant rejection by the targeted detection of enzymes and small molecules. In particular, cyanine dyes based on a FRET strategy and semi-cyanine dyes (HD/CS) based on an ICT strategy are the most widely used designs of fluorescent probes for the detection of immune-related signaling molecules and have shown significant results in preclinical models of tumors, immuno-inflammation, and transplant rejection.

From the perspective of clinical immunology, immune system abnormalities, which involve multiple disciplines and occur in multiple populations, lead to multiple diseases and serious consequences. Although a series of basic studies have been carried out regarding early diagnosis and treatment using organic fluorescent probes, there are still many problems that need to be solved, such as the penetration depth, bio-compatibility and biosafety of the fluorescent materials. In addition to further improving the performance of organic fluorescent materials, clear and specific targets for immune processes are still lacking. Combining chemical structure innovation with immunology can create a new generation of sophisticated tools that are more adaptable to medical technology and clinical settings, facilitating the further development of precision medicine (Table 1).

Author contributions

We strongly encourage authors to include author contributions and recommend using CRediT for standardised contribution descriptions. Please refer to our general author guidelines for more information about authorship.

Conflicts of interest

There are no conflicts to declare.

Acknowledgements

This work was supported by the NSFC (No. 22074036) and Special Funds for the Construction of the Science and Technology Project of Hunan Province (No. 2021RC4021), the Natural Science Foundation of Hunan Province (2023JJ20004).

Notes and references

1 M. Pasparakis, I. Haase and F. O. Nestle, Mechanisms regulating skin immunity and inflammation, *Nat. Rev. Immunol.*, 2014, **14**, 289–301.
2 D. Lobo-Silva, G. M. Carriche, A. G. Castro, S. Roque and M. Saraiva, Balancing the immune response in the brain: IL-10 and its regulation, *J. Neuroinflammation*, 2016, **13**, 297.
3 S. S. Chavan, V. A. Pavlov and K. J. Tracey, Mechanisms and Therapeutic Relevance of Neuro-immune Communication, *Immunity*, 2017, **46**, 927–942.
4 T. Krausgruber, N. Fortelny, V. Fife-Gernedl, M. Senekowitsch, L. C. Schuster, A. Lercher, A. Nemc, C. Schmidl, A. F. Rendeiro, A. Bergthaler and C. Bock, Structural cells are key regulators of organ-specific immune responses, *Nature*, 2020, **583**, 296–302.

5 M. W. Robinson, C. Harmon and C. O'Farrelly, Liver immunology and its role in inflammation and homeostasis, *Cell. Mol. Immunol.*, 2016, **13**, 267–276.
6 H. Hu, Y. Chen, S. Tan, S. Wu, Y. Huang, S. Fu, F. Luo and J. He, The Research Progress of Antiangiogenic Therapy, Immune Therapy and Tumor Microenvironment, *Front. Immunol.*, 2022, **13**, 802846.
7 Y. Zhang and Z. Zhang, The history and advances in cancer immunotherapy: understanding the characteristics of tumor-infiltrating immune cells and their therapeutic implications, *Cell. Mol. Immunol.*, 2020, **17**, 807–821.
8 D. S. Vinay, E. P. Ryan, G. Pawelec, W. H. Talib, J. Stagg, E. Elkord, T. Lichtor, W. K. Decker, R. L. Whelan, H. M. C. S. Kumara, E. Signori, K. Honoki, A. G. Georgakilas, A. Amin, W. G. Helferich, C. S. Boosani, G. Guha, M. R. Ciriolo, S. Chen, S. I. Mohammed, A. S. Azmi, W. N. Keith, A. Bilsland, D. Bhakta, D. Halicka, H. Fujii, K. Aquilano, S. S. Ashraf, S. Nowsheen, X. Yang, B. K. Choi and B. S. Kwon, Immune evasion in cancer: Mechanistic basis and therapeutic strategies, *Semin. Cancer Biol.*, 2015, **35**, S185–S198.
9 D. Bayik and J. D. Lathia, Cancer stem cell–immune cell crosstalk in tumour progression, *Nat. Rev. Cancer*, 2021, **21**, 526–536.
10 E. H. Koo, H. R. Jang, J. E. Lee, J. B. Park, S.-J. Kim, D. J. Kim, Y.-G. Kim, H. Y. Oh and W. Huh, The impact of early and late acute rejection on graft survival in renal transplantation, *Kidney Res. Clin. Pract.*, 2015, **34**, 160–164.
11 S. Thapa and X. Cao, Nervous regulation: beta-2-adrenergic signaling in immune homeostasis, cancer immunotherapy, and autoimmune diseases, *Cancer Immunol., Immunother.*, 2023, **72**, 2549–2556.
12 C. Zhang and K. Pu, Molecular and nanoengineering approaches towards activatable cancer immunotherapy, *Chem. Soc. Rev.*, 2020, **49**, 4234–4253.
13 C. Zhang and K. Pu, Organic sonodynamic materials for combination cancer immunotherapy, *Adv. Mater.*, 2023, DOI: **10.1002/adma.202303059**.
14 L. Mendive-Tapia and M. Vendrell, Activatable Fluorophores for Imaging Immune Cell Function, *Acc. Chem. Res.*, 2022, **55**(8), 1183–1193.
15 E. M. Rottenberg, Effective CPR at high altitudes likely requires oxygen-supplemented continuous abdominal compressions, *Am. J. Emerg. Med.*, 2014, **32**, 1545–1546.
16 S. Jang, E.-J. Kwon and J. J. Lee, Rheumatoid Arthritis: Pathogenic Roles of Diverse Immune Cells, *Int. J. Mol. Sci.*, 2022, **23**, 905.
17 J. V. Frangioni, New Technologies for Human Cancer Imaging, *J. Clin. Oncol.*, 2008, **26**, 4012–4021.
18 S. A. Hilderbrand and R. Weissleder, Near-infrared fluorescence: application to *in vivo* molecular imaging, *Curr. Opin. Chem. Biol.*, 2010, **14**, 71–79.
19 X. Liu, L. Pan, K. Wang, W. Pan, N. Li and B. Tang, Imaging strategies for monitoring the immune response, *Chem. Sci.*, 2022, **13**, 12957–12970.
20 M. Iafrate and G. O. Fruhwirth, How Non-invasive *in vivo* Cell Tracking Supports the Development and Translation of Cancer Immunotherapies, *Front. Physiol.*, 2020, **11**, 154.
21 M. Yang, J. Fan, J. Du and X. Peng, Small-molecule fluorescent probes for imaging gaseous signaling molecules: current progress and future implications, *Chem. Sci.*, 2020, **11**, 5127–5141.
22 P. Cheng, S. He, C. Zhang, J. Liu and K. Pu, A Tandem-Locked Fluorescent NETosis Reporter for the Prognosis Assessment of Cancer Immunotherapy, *Angew. Chem.*, 2023, **62**, e202301625.
23 S. He, P. Cheng and K. Pu, Activatable near-infrared probes for the detection of specific populations of tumour-infiltrating leukocytes *in vivo* and in urine, *Nat. Biomed. Eng.*, 2023, **7**, 281–297.
24 J. Huang, P. Cheng, C. Xu, S. S. Liew, S. He, Y. Zhang and K. Pu, Chemiluminescent Probes with Long-Lasting High Brightness for *In Vivo* Imaging of Neutrophils, *Angew. Chem.*, 2022, **61**, e202203235.
25 Y. Xu, C. Li, X. Ma, W. Tuo, L. Tu, X. Li, Y. Sun, P. J. Stang and Y. Sun, Long wavelength–emissive Ru(II) metallacycle–based photosensitizer assisting *in vivo* bacterial diagnosis and antibacterial treatment, *Proc. Natl. Acad. Sci. U. S. A.*, 2022, **119**, e2209904119.
26 Y. Xu, C. Li, J. An, X. Ma, J. Yang, L. Luo, Y. Deng, J. S. Kim and Y. Sun, Construction of a 980 nm laser-activated Pt(II) metallacycle nanosystem for efficient and safe photo-induced bacteria sterilization, *Sci. China: Chem.*, 2022, **66**, 155–163.
27 Y. Jin, Y. Hong, C. Park and Y. Hong, Molecular Interactions of Autophagy with the Immune System and Cancer, *Int. J. Mol. Sci.*, 2017, **18**, 1694.
28 G. L. Beatty and W. L. Gladney, Immune escape mechanisms as a guide for cancer immunotherapy, *Clin. Cancer Res.*, 2015, **21**, 687–692.
29 R. Kalluri, The biology and function of fibroblasts in cancer, *Nat. Rev. Cancer*, 2016, **16**, 582–598.
30 W. Zou, Immunosuppressive networks in the tumour environment and their therapeutic relevance, *Nat. Rev. Cancer*, 2005, **5**, 263–274.
31 J. Li, K. Chen, H. Liu, K. Cheng, M. Yang, J. Zhang, J. D. Cheng, Y. Zhang and Z. Cheng, Activatable near-infrared fluorescent probe for *in vivo* imaging of fibroblast activation protein-alpha, *Bioconjugate Chem.*, 2012, **23**, 1704–1711.
32 S. Y. Liu, H. Wang and G. Nie, Ultrasensitive Fibroblast Activation Protein-alpha-Activated Fluorogenic Probe Enables Selective Imaging and Killing of Melanoma *In Vivo*, *ACS Sens.*, 2022, **7**, 1837–1846.
33 C. Wu, Y. Mao, F. Zhang, X. Wang, N. Fan, W. Zhang, W. Zhang, P. Li and B. Tang, Uncovering the mechanism of cancer-associated fibroblasts induced immune evasion of hepatocellular carcinoma cells *via in situ* fluorescence imaging, *Sens. Actuators, B*, 2023, **389**, 133891.
34 A. Fernandez and M. Vendrell, Smart fluorescent probes for imaging macrophage activity, *Chem. Soc. Rev.*, 2016, **45**, 1182–1196.

35 S. E. Gill and W. C. Parks, Metalloproteinases and their inhibitors: regulators of wound healing, *Int. J. Biochem. Cell Biol.*, 2008, **40**, 1334–1347.
36 J.-O. Deguchi, M. Aikawa, C.-H. Tung, E. Aikawa, D.-E. Kim, V. Ntziachristos, R. Weissleder and P. Libby, Inflammation in Atherosclerosis, *Circulation*, 2006, **114**, 55–62.
37 F. A. Jaffer, D. E. Kim, L. Quinti, C. H. Tung, E. Aikawa, A. N. Pande, R. H. Kohler, G. P. Shi, P. Libby and R. Weissleder, Optical visualization of cathepsin K activity in atherosclerosis with a novel, protease-activatable fluorescence sensor, *Circulation*, 2007, **115**, 2292–2298.
38 A. Cobos-Correa, J. B. Trojanek, S. Diemer, M. A. Mall and C. Schultz, Membrane-bound FRET probe visualizes MMP12 activity in pulmonary inflammation, *Nat. Chem. Biol.*, 2009, **5**, 628–630.
39 E. R. Podack, Execution and suicide: cytotoxic lymphocytes enforce Draconian laws through separate molecular pathways, *Curr. Opin. Immunol.*, 1995, **7**, 11–16.
40 P. R. Hiebert and D. J. Granville, Granzyme B in injury, inflammation, and repair, *Trends Mol. Med.*, 2012, **18**, 732–741.
41 D. Masson, M. Nabholz, C. Estrade and J. Tschopp, Granules of cytolytic T-lymphocytes contain two serine esterases, *EMBO J.*, 1986, **5**, 1595–1600.
42 J. Huang, X. Chen, Y. Jiang, C. Zhang, S. He, H. Wang and K. Pu, Renal clearable polyfluorophore nanosensors for early diagnosis of cancer and allograft rejection, *Nat. Mater.*, 2022, **21**, 598–607.
43 R. Vanholder, B. Domínguez-Gil, M. Busic, H. Cortez-Pinto, J. C. Craig, K. J. Jager, B. Mahillo, V. S. Stel, M. O. Valentin, C. Zoccali and G. C. Oniscu, Organ donation and transplantation: a multi-stakeholder call to action, *Nat. Rev. Nephrol.*, 2021, **17**, 554–568.
44 P. Cheng, R. Wang, S. He, P. Yan, H. Huang, J. Chen, J. Shen and K. Pu, Artificial Urinary Biomarkers for Early Diagnosis of Acute Renal Allograft Rejection, *Angew. Chem.*, 2023, **62**, e202306539.
45 Q. D. Mac, D. V. Mathews, J. A. Kahla, C. M. Stoffers, O. M. Delmas, B. A. Holt, A. B. Adams and G. A. Kwong, Non-invasive early detection of acute transplant rejection *via* nanosensors of granzyme B activity, *Nat. Biomed. Eng.*, 2019, **3**, 281–291.
46 A. Mukherjee, P. C. Saha, R. S. Das, T. Bera and S. Guha, Acidic pH-Activatable Visible to Near-Infrared Switchable Ratiometric Fluorescent Probe for Live-Cell Lysosome Targeted Imaging, *ACS Sens.*, 2021, **6**, 2141–2146.
47 H. M. Khojah, S. Ahmed, M. S. Abdel-Rahman and A. B. Hamza, Reactive oxygen and nitrogen species in patients with rheumatoid arthritis as potential biomarkers for disease activity and the role of antioxidants, *Free Radical Biol. Med.*, 2016, **97**, 285–291.
48 G. Yang, C. C. Chang, Y. Yang, L. Yuan, L. Xu, C. T. Ho and S. Li, Resveratrol Alleviates Rheumatoid Arthritis *via* Reducing ROS and Inflammation, Inhibiting MAPK Signaling Pathways, and Suppressing Angiogenesis, *J. Agric. Food Chem.*, 2018, **66**, 12953–12960.
49 W. Song, W. Zhang, L. Yue and W. Lin, Revealing the Effects of Endoplasmic Reticulum Stress on Ferroptosis by Two-Channel Real-Time Imaging of pH and Viscosity, *Anal. Chem.*, 2022, **94**, 6557–6565.
50 C. Zhang, Z. Qiu, L. Zhang, Q. Pang, Z. Yang, J. K. Qin, H. Liang and S. Zhao, Design and synthesis of a ratiometric photoacoustic imaging probe activated by selenol for visual monitoring of pathological progression of autoimmune hepatitis, *Chem. Sci.*, 2021, **12**, 4883–4888.
51 E. S. Lee, H. Ko, C. H. Kim, H.-C. Kim, S.-K. Choi, S. W. Jeong, S.-G. Lee, S.-J. Lee, H.-K. Na, J. H. Park and J. M. Shin, Disease-microenvironment modulation by bare- or engineered-exosome for rheumatoid arthritis treatment, *Biomater. Res.*, 2023, **27**, 81.
52 P. Wei, W. Yuan, F. Xue, W. Zhou, R. Li, D. Zhang and T. Yi, Deformylation reaction-based probe for *in vivo* imaging of HOCl, *Chem. Sci.*, 2018, **9**, 495–501.
53 P. Wu, Y. Zhu, L. Chen, Y. Tian and H. Xiong, A Fast-Responsive OFF-ON Near-Infrared-II Fluorescent Probe for *In Vivo* Detection of Hypochlorous Acid in Rheumatoid Arthritis, *Anal. Chem.*, 2021, **93**, 13014–13021.
54 W. Chen, H. Liu, F. Song, L. Xin, Q. Zhang, P. Zhang and C. Ding, pH-Switched Near-Infrared Fluorescent Strategy for Ratiometric Detection of ONOO(−) in Lysosomes and Precise Imaging of Oxidative Stress in Rheumatoid Arthritis, *Anal. Chem.*, 2023, **95**, 1301–1308.
55 N. Shimasaki, A. Jain and D. Campana, NK cells for cancer immunotherapy, *Nat. Rev. Drug Discovery*, 2020, **19**, 200–218.
56 B. M. Larimer, E. Wehrenberg-Klee, F. Dubois, A. Mehta, T. Kalomeris, K. Flaherty, G. Boland and U. Mahmood, Granzyme B PET Imaging as a Predictive Biomarker of Immunotherapy Response, *Cancer Res.*, 2017, **77**, 2318–2327.
57 J. Xie, F. El Rami, K. Zhou, F. Simonetta, Z. Chen, X. Zheng, M. Chen, P. B. Balakrishnan, S.-Y. Dai, S. Murty, I. S. Alam, J. Baker, R. S. Negrin, S. S. Gambhir and J. Rao, Multiparameter Longitudinal Imaging of Immune Cell Activity in Chimeric Antigen Receptor T Cell and Checkpoint Blockade Therapies, *ACS Cent. Sci.*, 2022, **8**, 590–602.
58 Y. Zhang, S. He, W. Chen, Y. Liu, X. Zhang, Q. Miao and K. Pu, Activatable Polymeric Nanoprobe for Near-Infrared Fluorescence and Photoacoustic Imaging of T Lymphocytes, *Angew. Chem.*, 2021, **60**, 5921–5927.
59 W. A. Boivin, D. M. Cooper, P. R. Hiebert and D. J. Granville, Intracellular *versus* extracellular granzyme B in immunity and disease: challenging the dogma, *Lab. Invest.*, 2009, **89**, 1195–1220.
60 A. V. Sintsov, E. I. Kovalenko and M. A. Khanin, Apoptosis induced by granzyme B, *Russ. J. Bioorg. Chem.*, 2008, **34**, 647–654.
61 D. B. Kiselevsky, Granzymes and Mitochondria, *Biochemistry*, 2020, **85**, 131–139.
62 D. Johnson, Noncaspase proteases in apoptosis, *Leukemia*, 2000, **14**, 1695–1703.
63 M. Barry and R. C. Bleackley, Cytotoxic T lymphocytes: all roads lead to death, *Nat. Rev. Immunol.*, 2002, **2**, 401–409.

64 C. Y. Kadam and S. A. Abhang, Apoptosis Markers in Breast Cancer Therapy, *Adv. Clin. Chem.*, 2016, **74**, 143–193.
65 N. Anh, R. Anujan, K. Sahana, N. Dipika, B. Anthony, W. Alexandria, P. Leonid, O. Barbara and A. K. Ashish, Granzyme B nanoreporter for early monitoring of tumor response to immunotherapy, *Sci. Adv.*, 2020, **6**, eabc2777.
66 N. Sobhani, D. R. Tardiel-Cyril, A. Davtyan, D. Generali, R. Roudi and Y. Li, CTLA-4 in Regulatory T Cells for Cancer Immunotherapy, *Cancers*, 2021, **13**, 1440.
67 M. Chen, K. Zhou, S. Y. Dai, S. Tadepalli, P. B. Balakrishnan, J. Xie, F. E. I. Rami, T. Dai, L. Cui, J. Idoyaga and J. Rao, *In vivo* bioluminescence imaging of granzyme B activity in tumor response to cancer immunotherapy, *Cell Chem. Biol.*, 2022, **29**, 1556–1567.
68 S. A. Rosenberg and N. P. Restifo, Adoptive cell transfer as personalized immunotherapy for human cancer, *Science*, 2015, **348**, 62–68.
69 L. Zhu, X. J. Li, S. Kalimuthu, P. Gangadaran, H. W. Lee, J. M. Oh, S. H. Baek, S. Y. Jeong, S.-W. Lee, J. Lee and B.-C. Ahn, Natural Killer Cell (NK-92MI)-Based Therapy for Pulmonary Metastasis of Anaplastic Thyroid Cancer in a Nude Mouse Model, *Front. Immunol.*, 2017, **8**, 816.
70 J. I. Scott, S. Gutkin, O. Green, E. J. Thompson, T. Kitamura, D. Shabat and M. Vendrell, A Functional Chemiluminescent Probe for *in Vivo* Imaging of Natural Killer Cell Activity Against Tumours, *Angew. Chem.*, 2021, **60**, 5699–5703.
71 S. He, J. Li, Y. Lyu, J. Huang and K. Pu, Near-Infrared Fluorescent Macromolecular Reporters for Real-Time Imaging and Urinalysis of Cancer Immunotherapy, *J. Am. Chem. Soc.*, 2020, **142**, 7075–7082.
72 J. Lieberman, The ABCs of granule-mediated cytotoxicity: new weapons in the arsenal, *Nat. Rev. Immunol.*, 2003, **3**, 361–370.
73 Z. Cheng, E. J. Thompson, L. Mendive-Tapia, J. I. Scott, S. Benson, T. Kitamura, A. Senan-Salinas, Y. Samarakoon, E. W. Roberts, M. A. Arias, J. Pardo, E. M. Galvez and M. Vendrell, Fluorogenic Granzyme A Substrates Enable Real-Time Imaging of Adaptive Immune Cell Activity, *Angew. Chem.*, 2023, **62**, e202216142.
74 I. Voskoboinik, J. C. Whisstock and J. A. Trapani, Perforin and granzymes: function, dysfunction and human pathology, *Nat. Rev. Immunol.*, 2015, **15**, 388–400.
75 Y. Chen, Z. Zhou and W. Min, Mitochondria, Oxidative Stress and Innate Immunity, *Front. Physiol.*, 2018, **9**, 1487.
76 A. Mantovani, F. Marchesi, A. Malesci, L. Laghi and P. Allavena, Tumour-associated macrophages as treatment targets in oncology, *Nat. Rev. Clin. Oncol.*, 2017, **14**, 399–416.
77 A. Ramesh, S. Kumar, A. Brouillard, D. Nandi and A. Kulkarni, A Nitric Oxide (NO) Nanoreporter for Noninvasive Real-Time Imaging of Macrophage Immunotherapy, *Adv. Mater.*, 2020, **32**, e2000648.
78 X. Li, H. Chen, Y. Wang, H. Chen and Y. Gao, BODIPY-Based NO Probe for Macrophage-Targeted Immunotherapy Response Monitoring, *Anal. Chem.*, 2023, **95**, 7320–7328.
79 Y. Huo, J. Miao, Y. Li, Y. Shi, H. Shi and W. Guo, Aromatic primary monoamine-based fast-response and highly specific fluorescent probes for imaging the biological signaling molecule nitric oxide in living cells and organisms, *J. Mater. Chem. B*, 2017, **5**, 2483–2490.
80 N. Liao, L. Su, Y. Zheng, B. Zhao, M. Wu, D. Zhang, H. Yang, X. Liu and J. Song, *In Vivo* Tracking of Cell Viability for Adoptive Natural Killer Cell-Based Immunotherapy by Ratiometric NIR-II Fluorescence Imaging, *Angew. Chem.*, 2021, **60**, 20888–20896.